DOI: 10.1002/adma.200602311

Graded-Bandgap Quantum-Dot-Modified Nanotubes: A Sensitive Biosensor for Enhanced Detection of DNA Hybridization**

By *Chuan-Liang Feng*, *Xinhua Zhong*, *Martin Steinhart*, *Anne-Marie Caminade*, *Jean-Pierre Majoral*, and *Wolfgang Knoll**

Biosensors containing quantum dots (QDs) as fluorescent markers have been employed for immunoassays, gene expression, genomic analysis, and fluorescence imaging[1] because QDs have superior properties to traditional organic fluorophores, such as higher quantum yield and much sharper emission spectra.[2] Recently, the use of QDs as fluorescence resonance energy transfer (FRET) donors to detect DNA, RNA, or proteins[3] was reported, where an amplification of the detected fluorescent signal was achieved by exploiting FRET. One particularly promising strategy in this context involves funneling energy from strongly light-harvesting species towards a reaction center, because energy is always transferred from a species with a larger bandgap to a species with a smaller bandgap.[4] In this way, a cascaded-energy-transfer structure based on QD assembly has been constructed with a high photoluminescence (PL) intensity originating from the center layer.[5]

The use of QDs as biomarkers to functionalize nanotubes (NTs) has been also reported,[6] as a new and active field of research. It is known that the preparation of functionalized NTs, for example, inside an ordered porous alumina membrane,[7] can yield hybrid systems containing a large number of aligned and functionalized channels for biological applications.[8] For example, NTs functionalized with QDs have found promising applications as drug carriers, biomarkers, and biosensors.[6] Hence, taking advantage of the superior properties of QDs described above, we describe in this Communication a novel approach to designing functionalized NTs with a cascaded-energy-transfer architecture by incorporating graded-bandgap QDs into ordered porous alumina membranes (Scheme 1) and their use as highly sensitive biosensor component for the detection of DNA hybridization through energy transfer.

The incorporation of QDs into the NTs was performed by the well-known approach of layer-by-layer (LBL) deposition.[9] Mercaptoundecanoic acid (MPA) ligand coated ZnCdSe alloy QDs with luminescence maxima at $\lambda = 561$ nm (QD^{561}) ($d = 6.6$ nm), 594 nm (QD^{594}) ($d = 6.1$ nm), and 614 nm (QD^{614}) ($d = 5.5$ nm) were used.[10] Their PL emission and UV absorption spectra of aqueous suspensions are shown in Figure 1A and Figure S1 (Supporting Information), respectively. Several advantages of ZnCdSe alloy QDs compared with other types of QDs, for example, core/shell QDs, are summarized here:[11] 1) There are very few surface defects around the luminescent particles owing to the high crystallinity. 2) They have large particle sizes, hardened lattice structures, and decreased interdiffusion. 3) ZnCdSe alloy QDs can produce atomically abrupt jumps in the chemical potential, which can further localize free exciton states in the alloy crystallites. Therefore, the fluorescence stability of ZnCdSe alloy QDs can be greatly improved.

As a matrix forming the walls of the NTs we used globular N,N-disubstituted hydrazine phosphorus-containing dendrimers of the fourth generation having 96 terminal groups with either cationic $[G_4(NH^+Et_2Cl^-)_{96}]$ (G_4^+) or anionic $[G_4(CH\text{-}COO^-Na^+)_{96}]$ (G_4^-) character.[12] The two dendrimers possess a controlled shape and well-defined external and internal surfaces. The multilayer structures consisting of the two dendritic polyelectrolytes show a lower degree of interpenetration than multilayer systems composed of common linear polyelectrolytes. Therefore, they are ideal components for constructing compartmentalized NT walls, in which different functional species, such as water-soluble QDs with different size or composition in the case of the alloy particles used in this experiment, can be deposited with high spatial precision.[13]

For LBL deposition in an ordered porous alumina membrane, the pore walls were first coated with the positively charged 3-aminopropyl dimethylethoxysilane (3-APS), further allowing the deposition of a negatively charged den-

[*] Prof. W. Knoll, Dr. C.-L. Feng
Max Planck Institute for Polymer Research
Ackermannweg 10, 55128 Mainz (Germany)
E-mail: knoll@mpip-mainz.mpg.de
Prof. X. H Zhong
Department of Chemistry
East China University of Science and Technology
200237 Shanghai (P.R. China)
Dr. M. Steinhart
Max Planck Institute of Microstructure Physics
Weinberg 2, 06120 Halle (Germany)
Dr. A.-M. Caminade, Prof. J.-P. Majoral
Laboratoire de Chimie de Coordination, CNRS
205 Route de Narbonne, 31077 Toulouse Cedex 4 (France)

[**] Helpful discussions with T. Basché are gratefully acknowledged. Financial support came from the Deutsche Forschungsgemeinschaft (partly through SFB 625: "Von einzelnen Molekülen zu nanoskopisch strukturierten Materialien", and partly through CERC3, Mu 334/22-2: "A building-block approach for the study of transport and mechanism in confined environment: from synthesis to nano-organized design through controlled assembly"). Supporting Information is available online from Wiley or from the author.

ADVANCED MATERIALS

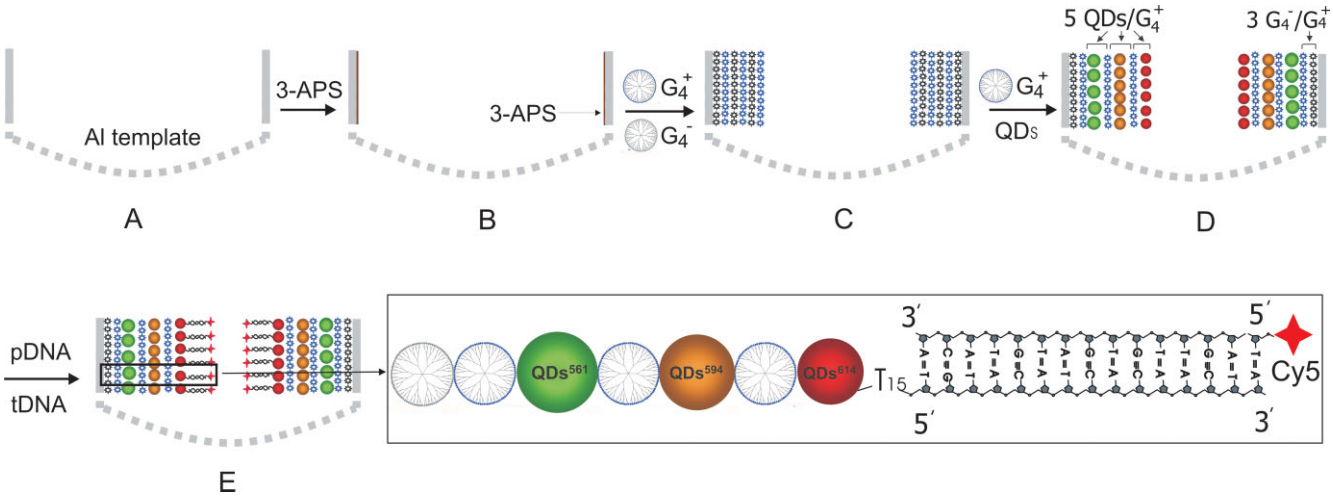

Scheme 1. Schematic of the NTs containing a graded-bandgap structure prepared by incorporating three types of ZnCdSe alloy QDs. A) Self-assembled porous alumina membrane is used as a template. B) The pore walls are coated with 3-aminopropyl dimethylethoxysilane (3-APS) to provide a positively charged surface. C) The first negatively charged dendrimer layer is deposited, followed by alternate deposition of positively and negatively charged dendrimers. Before the first QD layer is deposited, three bilayers of positively and negatively charged dendrimers are deposited. D) The assembly of QDs inside the template started with the deposition of QDs with luminescence maximum at $\lambda = 561$ nm (QD^{561}, green), then QDs with luminescence maximum at $\lambda = 594$ nm (QD^{594}, orange), and finally QDs with luminescence maximum at $\lambda = 614$ nm (QD^{614}, red). Five positively charged dendrimer/QD bilayers for each. E) After activation by *N*-hydroxysuccinimide (NHS) / 1-ethyl-3-(dimethylamino)propylcarbodiimide (EDC), probe DNA (pDNA) immobilization and hybridization with Cy5-labeled complementary DNA (tDNA) can be achieved inside the NTs (see enlargement).

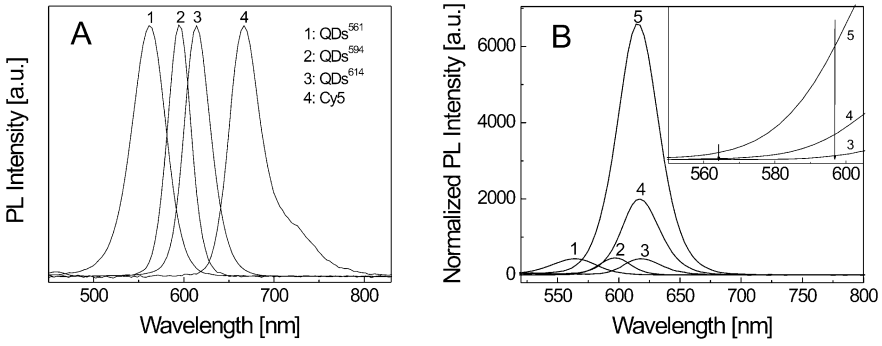

Figure 1. A) PL emission spectra of QD^{561}- (1), QD^{594}- (2), QD^{614}- (3), and Cy5-labeled (4) target DNA in aqueous solution. An excitation wavelength of $\lambda = 460$ nm was used for all the QDs and $\lambda = 630$ nm for Cy5. B) PL emission spectra of NT1, containing QD^{561} (1), NTs2, containing QD^{594} (2), NT3, containing QD^{614} (3), NT4, containing QD^{594} and QD^{614} (4), and NT5, containing QD^{561}, QD^{594}, and QD^{614} (5). Inset: Enlargement of the PL spectra in the short-wavelength region of NT3, NT4, and NT5. The peaks of the spectra were normalized to the absorption of the NTs at $\Lambda = 460$ nm of the different types of NTs shown in Figure S2 (Supporting Information).

drimer layer. Then, alternating layers of the positively charged dendrimers and negatively charged dendrimers or QDs were achieved by LBL deposition. Considering the quenching that occurs between the QDs and the pore walls,[14] three bilayers of oppositely charged dendrimers were assembled before the first QD layer was deposited in our experiments. Afterwards, the positively charged dendrimers and negatively charged QDs were deposited alternately. This cycle was repeated five times for each type of QD. In the final step, negatively charged QDs that formed the inner surface of the NTs were deposited for further functionalization (Scheme 1).

Three types of NTs containing a single type of QD (NT1 containing QD^{561}, NT2 containing QD^{594}, and NT3 containing QD^{614}) were first prepared; their PL emission spectra are shown in Figure 1B. As expected, the emission maxima of the NTs appear at wavelengths of around $\lambda = 561$, 594, and 614 nm (Fig. 1B, curves 1, 2, and 3), respectively. *No* spectral overlap from the template used is observed in these regions.[14] Then, NTs containing multiple types of QDs were prepared. To fabricate the NTs containing a cascaded-energy-transfer structure, the assembly of QDs inside the template started with the deposition of QDs with shorter emission wavelength (green) and proceeded to those with longer emission wavelength (red) (Scheme 1). Two kinds of such NTs, containing two (QD^{594}, QD^{614}; NT4) and three (QD^{561}, QD^{594}, QD^{614}; NT5) types of QDs, were prepared. Their normalized PL emission spectra are shown in Figure 1B (curves 4 and 5). It can be seen that they show exclusively an emission peak centered at $\lambda = 614$ nm, originating from QD^{614}. Comparing the intensity of the PL band at $\lambda = 614$ nm from the NT4 and NT5 gives an enhancement factor of ca. 4.1 and ca. 14, respectively, compared to that from the NT3. Here, much less emission from the QDs at shorter wavelength is observed (inset in Fig. 1B). A similar result has been reported for CdSe QDs by Franzl et al.[5]

The striking result above indicates that an efficient excitation energy transfer takes place from the larger bandgap QDs to the ones with lower band energy on the inner surface of the NTs. This occurs, first, because this sequence of QDs ensures sufficient spectral overlap between the different QD species for FRET to occur.[4] Second, this QD arrangement is characterized by a decrease of the bandgap energies from the outer to the inner surface of the NT walls. Therefore, hole and electron potentials in the walls of the NTs generate an intrinsic ramp for the energy transfer,[4] which is directed towards the center of the NTs. As discussed below, this is a key feature for the enhanced detection sensitivity of DNA hybridization inside the NTs.

To investigate the NTs with graded-bandgap architecture as potential biosensors for detecting DNA hybridization, amino-group-functionalized probe DNA with 30 nucleobases and Cy5-labeled complementary 15-mer DNA oligonucleotides were selected. (Cy5 is a reactive water soluble fluorescent dye of the cyanine dye family.) The NTs (NT3, NT4, and NT5) were first activated with *N*-hydroxysuccinimide (NHS)/1-ethyl-3-(dimethylamino)propylcarbodiimide (EDC), followed by the immobilization of probe DNA. Then, hybridization with Cy5-labeled target DNA was performed in the NTs. The measured, normalized PL emission spectra are shown in Figure 2A. An emerging shoulder of PL emission at about $\lambda = 670$ nm originating from Cy5 can just be observed beside the dominant peak at $\lambda = 614$ nm after DNA hybridization inside all the NTs. For NT3 (inset in Fig. 2A, curve 1), a small shoulder of PL emission appears beside the dominant peak at $\lambda = 614$ nm. The PL emission intensity of the Cy5 band significantly increases once QD^{594} and QD^{614} are incorporated (NT4, inset in Fig. 2A, curve 2) and is even larger if three types of QDs are present (NT5, inset in Fig. 2A, curve 3). It is found that this increase in the Cy5 emission is concomitant with the increase in PL intensity of the peak at $\lambda = 614$ nm. Hence, the increased Cy5 emission can be attributed to excitation energy transfers by FRET from the QDs to the Cy5.

In order to evaluate energy transfer efficiency from the QDs to the Cy5, the changes of the PL emission spectra induced by hybridization were analyzed. Figure 2B, curve 1 is the PL emission spectrum of NT5 before the hybridization; Figure 2B, curves 2 and 3 are the deconvoluted PL emission spectra of curve 3 in Figure 2A after hybridization in NT5. By measuring the PL intensity of curves 1 and 2 in Figure 2B at $\lambda = 614$ nm, we find that the PL emission intensity is reduced by ca. 3.2 % after DNA hybridization compared with before. Therefore, it can be concluded that the energy transfer occurs from the QDs to Cy5 and the energy transfer efficiency is expected to be ca. 3.2 %. Since the energy transfer efficiency strongly depends on the distance between donors and acceptors,[15] that from the QDs to Cy5 in the NTs can be further increased by using shorter chain length DNA or tuning the QD emission. Although the energy transfer efficiency from the QDs to Cy5 is relatively low here, it is already sufficient to ensure sensitive detection of DNA hybridization in the NTs. An enhancement factor of ca. 15 was found for the sensitivity in such types of NTs (Fig. S3). Direct comparison with DNA microarrays containing *no* cascaded-energy-transfer structure, for example, dendrimer-based DNA microarrays, was also performed. Only twofold detection sensitivity was reported for the dendrimer-based DNA microarrays.[16] The results suggest that NTs containing a cascaded-energy-transfer architecture have potential utility for the detection of trace amounts of DNA, owing to the enhancement in detection sensitivity, as reported for nanoparticles for biological detection.[17]

In conclusion, we have developed a versatile approach to designing functionalized NTs assembled with graded-bandgap ZnCdSe alloy QDs, which showed high sensitivity for detecting DNA hybridization. The enhancement in sensitivity afforded by the NTs provides the ability to confidently detect small but significant changes of the signal during biological detection. The detection sensitivity of the NTs was found to be tunable by varying the assemblies of gradient QDs inside the NTs. Tunable sensitivity in the NTs can also be expected by adjusting the distance between the QDs and DNA or tuning the QD emission. Taking advantage of the new optical and electrical properties achieved by the combination of size quantization and the gradient nature of the alloy QDs, NTs containing gradient QD assemblies may find a wide range of applications in various biomedical fields.

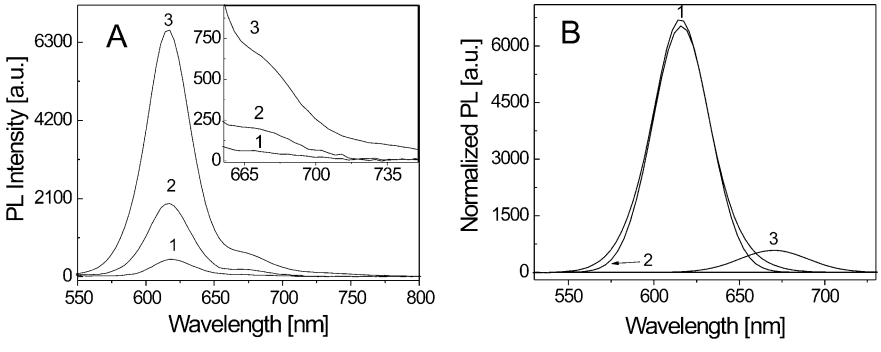

Figure 2. A) Normalized PL emission spectra of the NTs after hybridization with Cy5-labeled target DNA inside NT3, containing QD^{614} (1), NT4, containing QD^{594} and QD^{614} (2), and NT5, containing QD^{561}, QD^{594}, and QD^{614} (3). Inset: Enlargement of the PL spectra in the long-wavelength region. An additional shoulder of PL emission at $\lambda = 670$ nm, originating from Cy5, is observed beside the dominant peak at around $\lambda = 614$ nm for three different types of NTs after the hybridization. B) 1) The PL emission spectrum of NT5. 2,3) The deconvoluted PL emission spectra of NT5 after hybridization with Cy5-labeled DNA.

Experimental

The pore walls of the ordered porous alumina membranes (diameter 400 nm, depth 100 μm) were coated with 3-APS by placing the membranes in a closed glass vessel at 135 °C for 3 h. The first negatively charged dendrimer was deposited on the 3-APS from aqueous solution (1 mg mL^{-1}) for 50 min,

ADVANCED MATERIALS

followed by rinsing with Milli-Q water. The first positively charged dendrimer layer was then deposited from aqueous solution (1 mg mL^{-1}) for 50 min, followed by rinsing with Milli-Q water. The deposition of the positively charged dendrimers and negatively charged dendrimers or QDs (ca. 10^{-7} M) as a double layer was repeated until the desired number of multilayers was obtained.

The COOH groups of MPA-coated ZnCdSe alloy QDs were activated by immersion in an aqueous solution of 1 M EDC / 0.2 M NHS for 30 min. The amino-functionalized single-stranded DNA was covalently bonded on the inner walls of the NTs from a 1 μM aqueous solution (phosphate buffer (PB), pH 7.4) for 30 min, followed by rinsing with PB [18]. The aqueous solution containing Cy5-labeled target DNA (pH 7.4, 100 nM) was then applied to the NTs for 30 min at room temperature. After the NTs had been rinsed with PB and then Milli-Q water, DNA hybridization was detected by PL experiment. Probe DNA with 30-mer: 5′-TTT $(TTT)_4$ TGT ACA TCA CAA CTA-3′. Target DNA: 5′-Cy5-TAG TTG TGA TGT ACA-3′ (MWG-biotech AG, Ebersberg, Germany).

Absorption spectra were collected using a diode array UV-vis spectrometer Lambda 900, Perkin Elmer. PL emission spectra were collected using a FL3095SL, J&M TIDAS 9.5, Germany.

Received: October 10, 2006
Revised: February 26, 2007
Published online: June 29, 2007

[1] a) C. Y. Zhang, L. W. Johnson, *J. Am. Chem. Soc.* **2006**, *128*, 5324. b) P. Alivisatos, *Pure Appl. Chem.* **2000**, *72*, 3. c) W. W. Yu, E. Chang, R. Drezek, V. L. Colvin, *Biochem. Biophys. Res. Commun.* **2006**, *348*, 781.

[2] C. A. Leatherdale, W. K. Woo, F. V. Mikulec, M. G. Bawendi, *J. Phys. Chem. B* **2002**, *106*, 7619.

[3] a) I. L. Medintz, H. T. Uyeda, E. R. Goldman, H. Mattoussi, *Nat. Mater.* **2005**, *4*, 435. b) C. M. Niemeyer, *Angew. Chem. Int. Ed.* **2001**, *40*, 4128. c) A. R. Clapp, I. L. Medintz, J. M. Mauro, B. R. Fisher, M. G. Bawendi, H. Mattoussi, *J. Am. Chem. Soc.* **2004**, *126*, 301. d) M. Gruber, B. Wetzl, B. Oswald, J. Enderlein, O. S. Wolfbeis, *J. Fluoresc.* **2005**, *15*, 207.

[4] a) L. Sheeney-Haj-Khia, B. Basnar, I. Willner, *Angew. Chem. Int. Ed.* **2005**, *44*, 78. b) A. A. Mamedov, A. Belov, M. Giersig, N. N. Mamedova, N. A. Kotov, *J. Am. Chem. Soc.* **2001**, *123*, 7738. c) S. F. Wuister, R. Koole, C. de Mello Donega, A. Meijerink, *J. Phys. Chem. B* **2005**, *109*, 5504.

[5] T. Franzl, T. A. Klar, S. Schietinger, A. L. Rogach, J. Feldmann, *Nano Lett.* **2004**, *4*, 1599.

[6] a) D. L. Shi, J. Lian, W. Wang, G. K. Liu, P. He, Z. Y. Dong, L. Wang, R. C. Ewing, *Adv. Mater.* **2006**, *18*, 189. b) D. A. Heller, S. Baik, T. E. Eurell, M. S. Strano, *Adv. Mater.* **2005**, *17*, 2793.

[7] a) K. A. Williams, P. T. M. Veenhuizen, B. G. de la Torre, R. Eritja, C. Dekker, *Nature* **2002**, *420*, 761. b) A. V. Ellis, K. Vjayamohanan, R. Goswaimi, N. Chakrapani, L. S. Ramanathan, P. M. Ajayan, G. Ramanath, *Nano Lett.* **2003**, *3*, 279.

[8] a) H. Masuda, K. Fukuda, *Science* **1995**, *268*, 1466. b) Z. J. Liang, A. S. Susha, A. M. Yu, F. Caruso, *Adv. Mater.* **2003**, *15*, 1849. c) S. F. Ai, G. Lu, Q. He, J. B. Li, *J. Am. Chem. Soc.* **2003**, *125*, 11 140.

[9] a) G. Decher, J. D. Hong, *Ber. Bunsenges. Phys. Chem.* **1991**, *95*, 1430. b) T. Groth, A. Lendlein, *Angew. Chem. Int. Ed.* **2004**, *43*, 926.

[10] a) X. H. Zhong, R. Xie, Y. Zhang, T. Basché, W. Knoll, *Chem. Mater.* **2005**, *17*, 4038. b) M. Y. Gao, S. Kirstein, H. Möhwald, A. L. Rogach, A. Kornowski, A. Eychmüller, H. Weller, *J. Phys. Chem. B* **1998**, *102*, 8360.

[11] X. Zhong, M. Han, Z. Dong, T. J. White, W. Knoll, *J. Am. Chem. Soc.* **2003**, *125*, 8589.

[12] S. Merino, L. Brauge, A. M. Caminade, J. P. Majoral, D. Taton, Y. Gnanou, *Chem. Eur. J.* **2001**, *7*, 3095.

[13] D. H. Kim, P. Karan, P. Göring, J. Leclaire, A. M. Caminade, J. P. Majoral, U. Gösele, M. Steinhart, W. Knoll, *Small* **2005**, *1*, 99.

[14] J. Hohlbein, R. Rehn, R. B. Wehrspohn, *Phys. Status Solidi A* **2004**, *201*, 803.

[15] I. L. Medintz, S. A. Trammell, H. Mattoussi, J. M. Mauro, *J. Am. Chem. Soc.* **2004**, *126*, 30.

[16] a) V. Le-Berre, E. Trévisiol, A. Dagkessamanskaia, S. Sokol, A. M. Caminade, J. P. Majoral, B. Meunier, J. François, *Nucl. Acids Res.* **2003**, *31*, e88. b) E. Trevisiol, V. Leberre-Anton, J. Leclaire, G. Pratviel, A. M. Caminade, J. P. Majoral, J. M. François, B. Meunier, *New J. Chem.* **2003**, *27*, 1713.

[17] a) Y. W. C. Cao, R. C. Jin, C. A. Mirkin, *Science* **2002**, *297*, 1536. b) J. M. Nam, C. S. Thaxton, C. A. Mirkin, *Science* **2003**, *301*, 1884. c) P. Alivisatos, *Nat. Biotechnol.* **2004**, *22*, 47.

[18] C. L. Feng, G. J. Vancso, H. Schönherr, *Adv. Funct. Mater.* **2006**, *16*, 1306.

